

AdaFocus: Knowing When and Where to Look for Adaptive Visual Reasoning

Yuxiang Shen^{1,2,*} Hailong Huang^{3,†,*} Zhenkun Gao^{4,*} Xueheng Li^{1,2}
Chengjun Xie² Xuanhua He^{5,†} Jie Zhang^{2,†}

¹ University of Science and Technology of China ² Institute of Intelligent Machines, Hefei Institutes of Physical Science, CAS
³ Zhejiang University ⁴ East China Normal University ⁵ The Hong Kong University of Science and Technology

* Equal contribution † Corresponding authors ‡ Project Leader

Abstract

Multimodal Large Language Models (MLLMs) are shifting towards "Thinking with Images" by actively exploring image details. While effective, large-scale training is computationally expensive, which has spurred growing interest in lightweight, training-free solutions. However, existing training-free methods suffer from two flaws: perceptual redundancy from indiscriminate cropping, which adds overhead and noise; and a drift between semantic intent and spatial attention, which prevents accurate localization of user-focused regions. To address these challenges, we propose AdaFocus, a novel training-free framework designed for adaptive visual reasoning. AdaFocus follows a two-stage pipeline: a confidence-based module decides when to crop, and a semantic-guided localization module determines where to crop. This enables adaptive visual reasoning without additional training. Experimentally, AdaFocus delivers substantial performance gains while achieving approximately 4.0× speedup inference speedup than the SOTA method ZoomEyes, representing a significant advance in both accuracy and efficiency. Our code is publicly available at github.com/Xiaoxiang100/adafocus-final.

1 Introduction

In recent years, Multi-modal Large Language Models (MLLMs) (Bai et al., 2025; Wang et al., 2025b; Hurst et al., 2024; Comanici et al., 2025) have made significant progress in visual-language understanding (Gao et al., 2026). The prevailing paradigm, "Thinking about Images," (Li et al., 2024a) encodes images into static features and applies language-based reasoning mechanisms like Chain-of-Thought (Wei et al., 2022). However, this passive paradigm limits adaptive visual acquisition: inputs are uniformly resized or cropped to fixed resolutions, yielding static representations that cannot recover fine-grained details or adapt focus to reasoning demands (Li et al., 2025). As

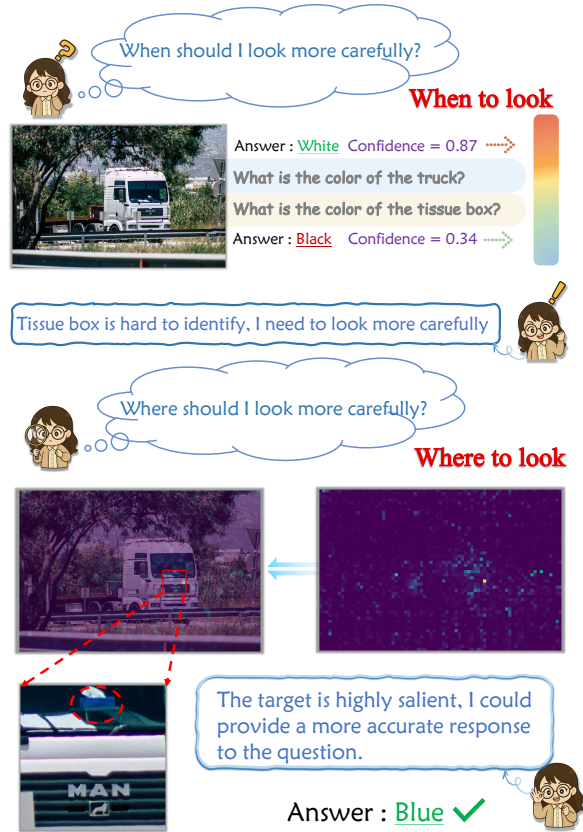


Figure 1: Illustration of AdaFocus: Enabling MLLMs to know when and where to look.

a result, performance degrades on tasks involving tiny targets. To address this limitation, a new paradigm termed "Thinking with Images" (OpenAI, 2025) has emerged, which empowers models with active perception capabilities (Su et al., 2025b,a; Liu et al., 2025). Unlike passive encoding, models can dynamically decide when and where to zoom, crop, or scan images in response to reasoning demands, as demonstrated by training-based approaches such as DeepEyes (Zheng et al., 2025) and V-Star (Hosseini et al., 2024). However, these training-based approaches require extensive computational resources and task-specific data, motivating the exploration of training-free alternatives

(Kim et al., 2025; Lee et al., 2025) that enable dynamic visual reasoning at inference time.

Recent training-free methods attempt to address this challenge through inference-time cost strategies. Existing methods, while generally adopting indiscriminate cropping, diverge into categories for acquiring fine-grained visual details: search-based methods (e.g., DC² (Wang et al., 2025c) and Zoom-Eye (Shen et al., 2025)), which iteratively evaluate regions but incur 5–10× inference overhead, and single-pass methods (e.g., MLLMs-Know (Zhang et al., 2025)), which rely on attention maps for efficient localization but often struggle with fine-grained tasks. These methods reflect two fundamental challenges: (1) determining *when* visual enhancement is necessary, as current methods indiscriminately crop all inputs without assessing information sufficiency; (2) identifying *where* to precisely localize targets, particularly in fine-grained multi-object scenarios. Together, these questions of when to look and where to look constitute the core challenges of training-free visual reasoning.

To validate these hypotheses and understand the underlying mechanisms, we conducted controlled experiments across multiple benchmarks, revealing two critical patterns (as shown in Sec 3.1).

Observation 1: Models Know When to Look, But Current Methods Don’t Ask. Existing methods uniformly crop all inputs under the assumption that finer details are always beneficial. However, our analysis shows that cropping degrades performance in some cases, as it often fails to add useful information for simple tasks and may instead introduce interfering noise, as shown in Figure 3. Additionally, we observe systematic differences in the model’s confidence distributions across tasks of varying difficulty, indicating that models inherently “know” when more information is needed, yet existing methods fail to leverage this signal. This motivates our confidence-based adaptive strategy for determining when cropping is necessary. Nevertheless, even when cropping is beneficial, current approaches still struggle with the challenge of precisely localizing targets.

Observation 2: Attention-based methods struggle with handling multi-object problems. While attention-based methods are efficient, they struggle with precise localization in multi-object scenarios. Attention maps highlight semantically relevant regions but often fail in multi-object settings, such as cropping only a single target or deviating from the intended regions. Figure 5 reveals that atten-

tion mechanisms capture “what is relevant” rather than “where each object is”. This motivates our semantic-guided localization that explicitly decouples language intent from visual attention to answer *where* to look. These findings expose a fundamental gap: existing methods treat visual enhancement as uniform, whereas effective reasoning requires adaptive decisions about both whether additional visual information is needed and where to precisely localize relevant regions.

Building on these insights, we propose AdaFocus, a training-free framework that addresses both dimensions. Unlike prior methods that uniformly crop all inputs, AdaFocus dynamically determines *when* cropping is beneficial and *where* to precisely localize targets. For the *when* decision, AdaFocus exploits intrinsic model confidence as a measure of information sufficiency, avoiding unnecessary and potentially noisy cropping when confidence is high. For the *where* decision, we introduce a semantic-guided multi-object localization mechanism that decouples semantic relevance from spatial positioning, enabling accurate localization in complex scenes. By integrating these adaptive decisions, AdaFocus achieves superior performance without iterative search overhead, consistently existing training-free methods with a 4.0× speedup across multiple benchmarks and generalizing effectively across diverse MLLM architectures.

Our contributions can be summarized as follows: (1) We identify two critical deficiencies in existing training-free methods through systematic empirical analysis: indiscriminate cropping that degrades performance, and attention-based localization that conflates semantic relevance with spatial precision. (2) We propose **AdaFocus**, a training-free framework enabling adaptive visual reasoning by determining *when* and *where* to crop through confidence-guided decision and semantic-guided localization. (3) Extensive experiments demonstrate that AdaFocus achieves superior accuracy across multiple benchmarks while delivering 4.0× speedup, generalizing effectively across diverse MLLMs architectures.

2 Related Work

2.1 Multimodal Large Language Models

Multimodal Large Language Models (MLLMs) have evolved from early end-to-end pre-training (Alayrac et al., 2022; Radford et al., 2021) to modular adaptation, in which pre-trained vision encoders are aligned with frozen LLMs via learnable con-

nectors, ranging from linear projections (Liu et al., 2023; Zhu et al., 2023) to more sophisticated Q-Formers (Dai et al., 2023). Despite their success, a critical bottleneck persists: fixed input resolution causes severe information loss for fine-grained details (Li et al., 2024b; Wu and Xie, 2024). Recent high-resolution models address this via dynamic resolution strategies, such as partitioning images into grids (e.g., LLaVA-NeXT (Liu et al., 2024), InternVL (Chen et al., 2024)) or natively scaling vision encoders (Bai et al., 2025). However, these methods process image patches passively and uniformly, failing to focus on task-relevant regions and thus wasting computation on background noise while missing critical details.

2.2 Vision-Language Reasoning

Recent work enables MLLMs to actively query visual content for fine-grained reasoning. Training-based approaches, such as DeepEyes (Zheng et al., 2025) and Pixel Reasoner (Wang et al., 2025a), internalize active perception through reinforcement learning or supervised trajectories, but incur high training costs and exhibit limited transferability to off-the-shelf MLLMs. In contrast, training-free methods simulate human-like zooming via iterative search; for example, ZoomEye (Shen et al., 2025) explores image details using hierarchical trees, but its multi-round inference introduces substantial latency. More efficient approaches, such as Vi-Crop (Zhang et al., 2025), leverage cross-attention for localization. However, they primarily address *where* to look but neglect *whether* cropping is actually needed, often adopting a noisy "always-crop" policy and performing poorly in complex multi-object scenarios.

In contrast, our framework unifies Token Confidence and Attention Maps. This synergy enables autonomous, decision-aware zooming. By determining necessity before action, we achieve the precision of search-based methods without their high latency, and the efficiency of attention-based methods without their redundancy.

3 Method

3.1 Analysis: When and Where to Look

Before introducing AdaFocus, we systematically analyze the fundamental limitations of existing training-free methods in determining *when* and *where* to crop. Our analysis aims to answer two critical questions: (1) Can models know when ad-

ditional visual information is necessary? (2) What causes attention-based localization to fail on fine-grained tasks?

Can MLLMs know when to look? In the **Thinking with Images** paradigm, some work enables models to decide **when to look** via reinforcement learning, whereas most training-free methods adopt indiscriminate cropping and re-encoding for all samples, neglecting the critical question of **when to crop or zoom**. For visually simple samples, such forced cropping incurs unnecessary computational overhead and inference latency, and can introduce redundant or noisy local information that misleads the model into incorrect answers. We present two representative examples in Figure 3.

Additional visual evidence is often expected to improve the prediction confidence of MLLMs. However, this assumption has not been systematically validated across different samples. To investigate this, we conduct a token-level confidence analysis before and after cropping. Based on the confidence change after cropping, we categorize samples into two exclusive groups: (i) *Need Processing*, where confidence increases ($Score_{crop} > Score_{org}$), and (ii) *No Need Processing*, where confidence remains unchanged or decreases ($Score_{crop} \leq Score_{org}$). The confidence distributions of the two groups are shown in Figure 2.

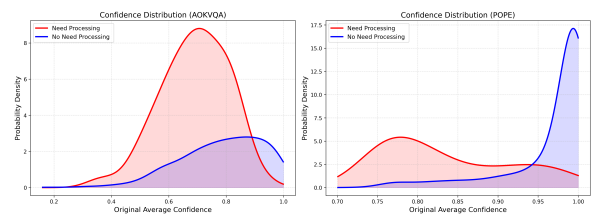


Figure 2: Probability density distributions of original average confidence

As shown in Figure 2, the *Need Processing* and *No Need Processing* samples exhibit a clear separation in their original average confidence distributions. On both AOKVQA and POPE, the *No Need Processing* samples show higher initial confidence, indicating that the original image provides sufficient visual evidence for prediction. In contrast, the *Need Processing* samples are concentrated in lower-confidence regions, suggesting that additional local visual information is more beneficial when the model’s initial prediction is uncertain.

This analysis reveals a heterogeneous effect of cropping on model confidence: while some samples benefit from additional visual details,

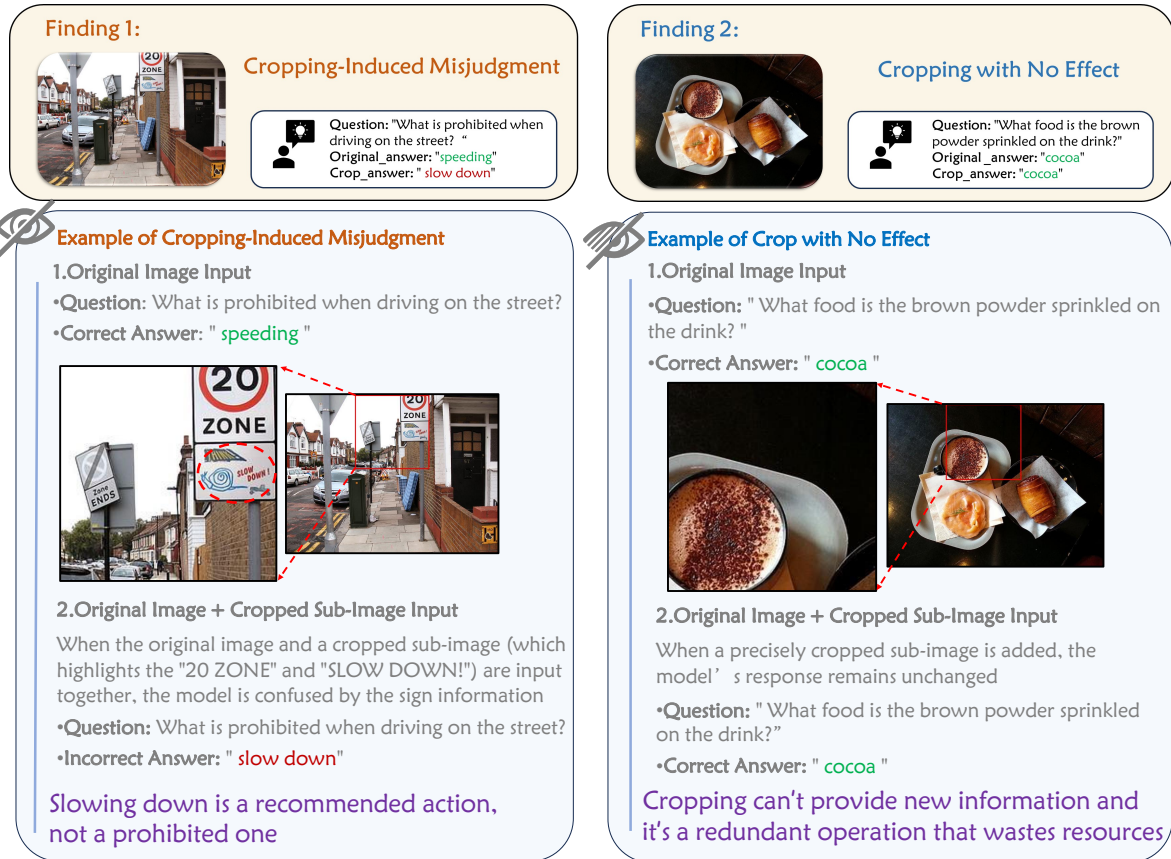


Figure 3: Limitations of indiscriminate cropping strategies

many show unchanged or even reduced confidence, which helps explain cases where originally correct predictions deteriorate after introducing extra cropped views. Importantly, the original confidence effectively reflects the model's need for additional visual evidence, enabling a simple and reliable criterion for deciding **when to look**.

Limitations of Attention Maps Multimodal large language models (MLLMs) inherently possess visual grounding capabilities (Zhang et al., 2025). The spatial attention enables efficient visual localization compared to search-based methods (e.g., DC² (Wang et al., 2025c) and Zoom-Eye (Shen et al., 2025)). However, relying on raw attention maps still faces two major challenges:

The first challenge is semantic disentanglement. For queries involving spatial relations (e.g., "Is the bicycle on the left or right side of the motorcycle?"), a single query embedding derived from the entire question often fails to distinguish multiple entities, resulting in diffused attention. We address this by using few-shot in-context learning (ICL) to extract the core semantic target, enabling more focused attention on the queried entity. The second challenge concerns dense multi-instance sep-

aration. For same-category multi-instance queries (e.g., "How many people?"), raw attention maps tend to merge nearby objects into contiguous regions. We mitigate this issue by applying attention thresholding to generate candidate boxes, followed by an NMS-inspired overlap filtering step to remove redundant regions. The model then produces the final answer using the refined visual evidence.

By integrating these two refinements, we convert the model's attention into a reliable mechanism for precise localization, effectively answering **where to look** even in complex scenes.

3.2 AdaFocus: Overview

To mitigate existing limitations, we propose AdaFocus, a training-free framework designed for efficient active perception. It operates through a unified pipeline comprising two key stages: (1) A confidence-based strategy for "When to look," which avoids redundant processing by assessing information sufficiency; and (2) A semantic-guided localization mechanism for "Where to look," which explicitly decouples semantic intent from spatial attention to ensure precise multi-object targeting. The overall workflow is illustrated in Figure 4.

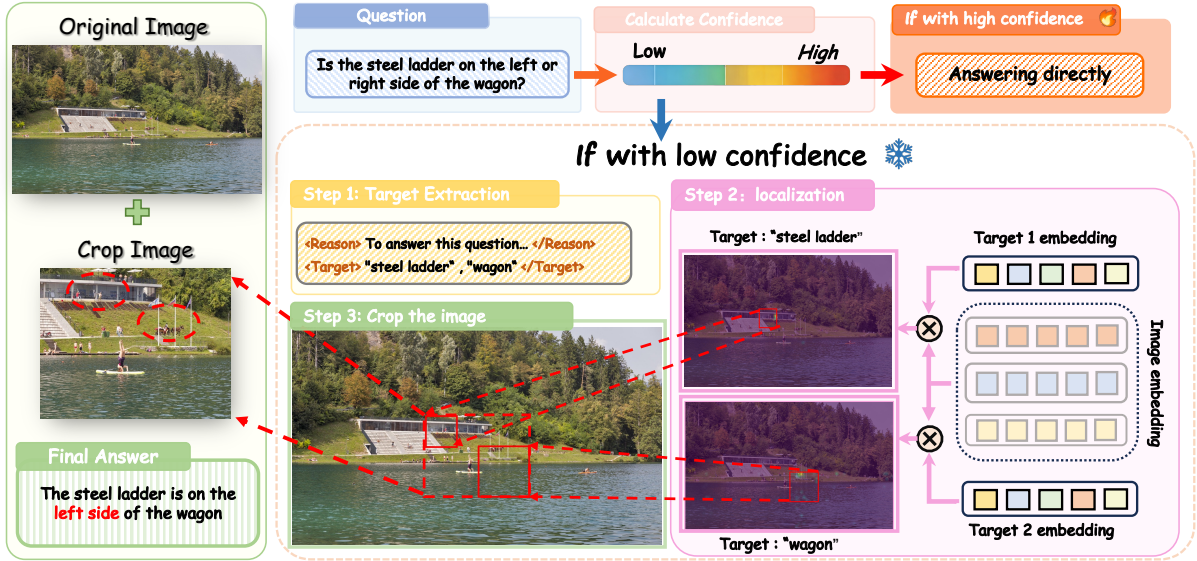


Figure 4: The overall workflow of the AdaFocus framework.

3.3 Confidence-based Cropping Strategy: "Determining When to look"

For a given input image I and query Q , the model first performs an initial inference to obtain a preliminary answer sequence, denoted as $Answer_{pre}$. However, relying solely on the global view may be insufficient for all fine-grained reasoning requirements. To strike an optimal balance between improving model performance and conserving computational resources, we design a confidence-based cropping strategy to determine whether to trigger a subsequent visual enhancement module.

Model Confidence Quantification. We quantify the model’s confidence by utilizing the average confidence of the tokens in the generated answer sequence. Specifically, the sequence is defined as

$$Y = \{y_1, y_2, \dots, y_T\}, \quad (1)$$

where y_t represents the t -th token, and $P(y_t|\cdot)$ denotes the probability of the model generating this token at step t . We define the confidence score C as the arithmetic mean of the Softmax probabilities of all tokens in the sequence. This confidence score C intuitively reflects the model’s uncertainty regarding the preliminary answer $Answer_{pre}$.

$$C = \frac{1}{T} \sum_{t=1}^T P(y_t|\cdot). \quad (2)$$

Optimal Threshold Selection. A simple yet effective approach is to use a fixed decision threshold

τ . As demonstrated in Section 4.6, applying cropping only to samples with confidence scores exceeding this threshold improves performance while reducing computational overhead.

When representative validation data are available and closely aligned with the test distribution, we further consider a principled threshold optimization strategy. Specifically, threshold selection is formulated as a statistical decision problem, where the optimal τ is obtained by maximizing the following utility function:

$$J_\lambda(\tau) = \text{TPR}(\tau) - \lambda \cdot \text{FPR}(\tau), \quad \lambda > 0. \quad (3)$$

Here, TPR and FPR denote the true positive rate and false positive rate, respectively, and λ serves as a cost-weighting hyperparameter that balances potential performance gains against unnecessary cropping. More details in Appendix D.

This optimization strategy assumes access to representative validation data. **In open-domain settings where such data cannot be reliably obtained, employing a high fixed threshold remains a stable and effective alternative**, as evidenced by the results in Table 5. These observations further demonstrate the robustness and generalization capability of our approach.

Final Decision Process. Based on the optimal decision boundary, we perform the following binary decision: (1) $C \geq \tau$: the model exhibits high confidence on the global view. In this case, we consider the available visual information sufficient for reasoning and directly output $Answer_{pre}$ as the

final answer. (2) $C < \tau$: the model shows uncertainty, indicating that the current visual information may be insufficient to support fine-grained reasoning. We therefore trigger the subsequent visual enhancement module.

3.4 Semantic-Guided Localization: “Determining Where to Crop”

Semantic Decoupling (What to Look). To accurately extract key visual entities, we employ a Few-Shot In-Context Learning strategy. We design a prompt template based on Chain-of-Thought. We guide the model to first generate a `<Reason>` tag before outputting the final `<target>`.

Formally, given a question Q , the model outputs a semantic target set $E = \{e_1, e_2, \dots\}$. For example, for "What kind of animal is on the red sign?", the model generates: `<Reason>`The question asks about something on a sign. The core subject to locate is the sign.`</Reason><Target>`red sign`</Target>`. Then it extracts $E = \{\text{"red sign"}\}$.

Spatial Attention Mapping (Where to Look). After identifying the semantic target E , we use the extracted `<target>` to construct a localization prompt. The process is as follows: Let Z_{img} and Z_{text} be the token sequences. We extract the attention matrix and calculate the average attention:

$$A_{\text{map}} = \text{Agg}(\text{Attn}(Z_{\text{text}} \rightarrow Z_{\text{img}})) \quad (4)$$

In this formulation, $\text{Agg}(\cdot)$ averages attention responses across all heads. Given the attention map A_{map} , we identify distinct salient regions using a multi-scale sliding window search that maximizes local attention contrast. These regions are then consolidated into a single union bounding box B_{union} . The original image I is then cropped and resized based on B_{union} to produce a detail-preserving local view I_{crop} .

Dealing with Multi-instances. For queries involving multiple instances of the same category (e.g., "How many people?"), we introduce an attention-based post-processing scheme to separate closely spaced targets. Specifically, an attention score threshold is applied to filter foreground regions, with high-response areas identified as candidate boxes. To remove highly overlapping boxes, we apply an NMS-inspired (Neubeck and Van Gool, 2006) deduplication step: boxes with an IoU greater than 0.5 are treated as duplicates and pruned. This process effectively reduces redun-

dancy, enabling accurate localization and counting of individual objects.

4 Experiments

4.1 Implementation Details

Experimental Setup. To validate the effectiveness of our approach, we integrate the AdaFocus framework with two widely-used open-source models: Qwen2.5VL-3B (Bai et al., 2025) and LLaVA-1.5-7B (Liu et al., 2023). We conduct a comprehensive comparison against both the original baselines and several state-of-the-art methods, including training-free approaches (e.g., ZoomEyes (Shen et al., 2025), MLLMs-Know (Zhang et al., 2025), DC² (Wang et al., 2025c), and ViCrop (Zhang et al., 2023)) and training-based models (e.g., PixelReasoner (Wang et al., 2025a)).

Datasets and Benchmarks. We evaluate our model across various dimensions using four benchmarks. First, we select **AOKVQA** (Schwenk et al., 2022) and **POPE** (Li et al., 2023) to assess general reasoning capabilities on knowledge-intensive tasks. Furthermore, to validate the effectiveness of our cropping strategy on fine-grained features, we introduce two challenging high-resolution datasets: **V*-Bench** (Wu and Xie, 2024) and **HR-Bench** (Wang et al., 2025c). Both benchmarks are rich in visual elements, posing a significant challenge to a model’s ability to capture minute details. Detailed settings regarding hyperparameters, prompts, and dataset statistics are provided in the Appendix.

4.2 Qualitative Analysis

Our method excels on benchmarks prioritizing visual distinctness (HR-Bench, V*-Bench). Despite LLaVA’s fixed resolution limiting attention granularity, we achieve substantial gains: **+11.25%** (HR-Bench 4K), **+9.87%** (8K), and **+14.12%** (V*-Bench). Leveraging the Qwen2.5-VL backbone, our model attains a state-of-the-art **70.00%** on HR-Bench 8K, outperforming the baseline by **11.12%** and ZoomEyes (65.63%) by a clear margin. These results confirm that semantic-guided localization effectively mitigates resolution bottlenecks by precisely identifying query-relevant regions.

For reasoning-heavy benchmarks (AOKVQA, POPE), improvements are moderate, indicating that the primary challenge here lies in logical deduction rather than visual recognition. However, the consistent boost, pushing Qwen2.5-VL to **73.10%** on AOKVQA, highlights the advantage of our

Model	Method	Training-free	AOKVQA	POPE	V* Bench	HR-Bench 4K	HR-Bench 8K
LLaVA-v1.5-7B	Baseline* (Liu et al., 2023)	✓	71.00	86.98	48.68	36.13	32.13
	DC ² (Wang et al., 2025c)	✓	-	-	57.60	-	39.50
	VisCrop (Zhang et al., 2023)	✓	-	-	62.30	46.25	35.75
	MLLMs-Know* (Zhang et al., 2025)	✓	72.31	87.25	56.02	44.38	37.25
	ZoomEyes (Shen et al., 2025)	✓	70.56	88.94	83.25	49.88	48.63
	Ours (AdaFocus)	✓	72.90	87.37	62.80	47.38	42.00
Δ vs. Baseline			+1.90	+0.39	+14.12	+11.25	+9.87
Qwen2.5VL-3B	Baseline* (Bai et al., 2025)	✓	71.44	87.20	75.90	67.50	58.88
	Pixel Reasoner (Wang et al., 2025a)	✗	-	-	84.82	-	66.00
	MLLMs-Know* (Zhang et al., 2025)	✓	71.62	89.12	75.90	66.36	64.88
	ZoomEyes (Shen et al., 2025)	✓	71.26	88.93	89.01	70.13	68.38
	Ours (AdaFocus)	✓	73.10	89.12	86.38	73.25	70.00
	Δ vs. Baseline			+1.66	+1.92	+10.48	+5.75

Table 1: **Comparison with state-of-the-art methods.** Highest results are marked in darker colors (Blue for LLaVA, Red for Qwen). The gray rows show the absolute improvement (Δ) of Ours over the Baseline. * Results are reproduced by us using official implementations.

confidence-based mechanism over indiscriminate zooming. By applying cropping *only when beneficial*, this strategy acts as a **semantic safeguard**: it clarifies local details without severing the global context. Overall, these findings show the flexibility of our approach: it effectively **overcomes resolution limits** in perception tasks while keeping the core meaning needed for complex reasoning. For further discussion on task-specific representation constraints and additional evaluations on Qwen3, please refer to Appendix G and Appendix F.

4.3 Qualitative Analysis

To visually demonstrate the effectiveness of our **Where to Look** mechanism, we compare the attention maps and final cropped regions generated by AdaFocus with those from a baseline attention-based localization method (MLLMs-Know).

Accurate multi-object localization: In Figure 5(A), the baseline suffers from a single-object bias, attending only to the ‘steel ladder’ while missing the ‘wagon’. In contrast, AdaFocus explicitly decouples multiple targets, activating both the ‘steel ladder’ and ‘wagon’. As shown in Figure 5(B), the resulting union of bounding boxes effectively covers both objects, providing the MLLM with a complete local view to accurately reason about their spatial relationship.

Robust target identification: In Figure 5(C), the baseline’s attention drifts to the dominant adult in the scene (incorrect target). Guided by our prompt-driven target extraction, AdaFocus accurately focuses on the "child", ensuring the cropped region aligns with the intended semantic target, as shown in Figure 5(D). These qualitative results demonstrate that our semantic-guided attention



Figure 5: comparison of localization precision.

mechanism significantly mitigates attention diffusion and semantic drift, ensuring that the "thinking with images" process relies on relevant visual evidence.

4.4 Efficiency analysis

Inference efficiency is an important factor for training-free methods. We evaluate AdaFocus against two representative baselines: **ZoomEyes** (the current SOTA) and **MLLMs-Know** (an attention-based method). ZoomEyes organizes the image into a hierarchical tree and performs iterative search to simulate zooming. Although effective,

this global traversal becomes increasingly expensive. As shown in Figure 6, processing HR-Bench 8K requires more than 10 hours.

In contrast, AdaFocus localizes informative regions directly from attention maps, avoiding exhaustive search over the full image. On HR-Bench 8K, this yields an approximately 4.0 \times speedup compared with ZoomEyes, while maintaining competitive performance.

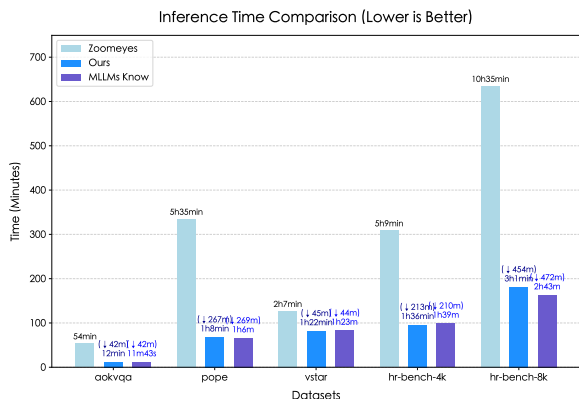


Figure 6: Comparison of total GPU inference time (in minutes) across different methods.

Furthermore, AdaFocus operates at a comparable speed to MLLMs-Know across all evaluated datasets. However, the accuracy differs substantially on challenging high-resolution benchmarks. For example, AdaFocus achieves 86.38% on V*-Bench and 70.00% on HR-Bench 8K, compared to 75.90% and 64.88% for MLLMs-Know, respectively. These results suggest that the improvement mainly comes from more effective allocation of computation, rather than increased inference cost.

4.5 Ablation study

4.5.1 Ablation on Cropping Strategy

Model	AOKVQA	V*-Bench
Qwen2.5VL-3B		
<i>w/o cropping strategy</i>	71.96%	85.86%
<i>w/ cropping strategy</i>	73.10%	86.38%
Δ	+1.14%	+0.52%

Table 2: Quantitative evaluation of cropping strategy.

As shown in Table 2, our adaptive cropping strategy consistently improves accuracy compared to indiscriminate cropping (*w/o cropping strategy*). For Qwen2.5-VL, our strategy yields a +1.14% boost on AOKVQA and +0.52% on V*-Bench. This confirms that indiscriminate cropping introduces

visual noise and misjudgments, which our selective strategy effectively avoids.

Benchmark	Acc	Time	Crop %
AOKVQA			
<i>w/o cropping strategy</i>	71.96	26m24s	100%
<i>w/ cropping strategy</i>	73.10	12m33s	32.40%
Δ	+1.14	-13m51s	-67.60%
V*-Bench			
<i>w/o cropping strategy</i>	85.86	1h04m	100%
<i>w/ cropping strategy</i>	86.38	1h18m	77.48%
Δ	+0.52	+14m	-22.52%

Table 3: Performance and efficiency comparison.

Table 3 demonstrates the efficiency of our confidence-based strategy. On AOKVQA, we skip redundant cropping for 67.60% of samples, cutting inference time by half. Notably, our adaptive approach is even more accurate than full cropping (+1.14), proving that it avoids the interference noise often introduced by unnecessary zooming. On complex tasks like V*-Bench, the model naturally crops more frequently but still reduces redundant processing by 22.52% while maintaining high accuracy. This shows AdaFocus adapts to task difficulty, achieving a superior balance between speed and performance.

4.5.2 Ablation on Localization Component

Model & Strategy	AOKVQA	POPE	V*-Bench	HR 4K	HR 8K
LLaVA-v1.5-7B					
<i>w/o Semantic-Guided Localization</i>	72.31%	87.25%	56.02%	44.38%	37.25%
<i>w/ Semantic-Guided Localization</i>	72.90%	87.37%	62.80%	47.38%	42.00%
Δ	0.59%	0.12%	6.78%	3.00%	4.75%
Qwen2.5VL-3B					
<i>w/o Semantic-Guided Localization</i>	71.62%	89.12%	75.90%	66.36%	64.88%
<i>w/ Semantic-Guided Localization</i>	71.96%	89.12%	85.86%	72.50%	70.00%
Δ	0.34%	-	9.96%	6.14%	5.12%

Table 4: Ablation on Semantic-Guided Localization.

To validate the Semantic-Guided Localization component, we evaluate model performance with and without this module (Table 4). The results reveal a clear pattern: while improvements on general reasoning tasks (AOKVQA, POPE) are marginal, the component yields substantial gains on high-resolution, detail-heavy benchmarks. For instance, Qwen2.5-VL achieves a +9.96% boost on V*-Bench and +6.14% on HR 4K, while LLaVA-v1.5 improves by +6.78% on V*-Bench. This demonstrates that explicitly guiding spatial attention with semantic targets effectively isolates query-relevant regions, which is crucial for localizing fine-grained details in complex scenes.

4.6 Confidence Sensitivity Analysis

To evaluate the robustness of our confidence-based cropping strategy, we conduct a sensitivity analysis aligned with the two scenarios introduced in subsection 3.3: optimizing the decision threshold via the utility function, and applying direct fixed thresholds for open-domain settings.

Threshold Optimization via Utility Function.

When validation data is available, we determine the optimal threshold τ by maximizing the utility function $J_\lambda(\tau)$. We analyze this optimization on AOKVQA by varying the cost-weighting hyperparameter λ . As shown in Table 5, the performance peaks at 73.10% when $\lambda = 1.5$, which derives an optimal threshold of $\tau = 0.734$. This confirms that our algorithm successfully finds a favorable trade-off between capturing fine-grained visual details and limiting computational redundancy.

Model	Baseline	Full Crop (All Crop)	Cropping Strategy (λ)			Fixed Thresh. ($\tau = 0.92$)
	(Original)		1.0	1.5	2.0	
Threshold (τ)	-	-	0.830	0.734	0.533	0.92
Qwen2.5-VL	71.44	71.96	72.58	73.10	72.49	72.05

Table 5: Sensitivity Analysis of cropping strategy.

Threshold Sensitivity in Open-Domain. In real-world open-domain scenarios, it is often impractical to carefully tune the hyperparameter λ . To evaluate whether our framework can still perform reliably without such tuning, we sweep across a range of threshold values τ (see Table 6). The results show that our method is not sensitive to the exact choice of the threshold. Even without precise calibration, the model maintains stable performance, and its accuracy consistently remains above the baseline across a wide range of relatively high thresholds (e.g., $\tau \in [0.94, 1.00]$).

Dataset	Base	<i>random</i>		<i>continuous</i>			
		0.80	0.90	0.94	0.96	0.98	1.00
HR-4K	67.50	72.75	72.50	72.75	72.50	72.50	72.50
HR-8K	58.88	68.25	69.88	70.00	70.00	70.00	70.00
V*-Bench	75.90	81.15	84.81	86.38	86.38	85.86	85.86
AOKVQA	71.44	72.31	72.40	72.23	72.23	72.14	71.97

Table 6: Sensitivity analysis across multiple benchmarks under varying confidence thresholds τ .

Robustness with a fixed Threshold. Building on the observed stability, we evaluate a single, conservative fixed threshold ($\tau = 0.96$) across all datasets without any per-task adjustment (Table 7). Under this strictly unified zero-shot setting,

AdaFocus consistently outperforms the baseline, achieving an average accuracy gain of **+9.35%**. Simultaneously, it bypasses redundant cropping to reduce processed image regions by an average of **10.63%**. This confirms that AdaFocus can function as a highly robust, plug-and-play module that adapts to diverse tasks using just a simple, high fixed threshold.

Benchmark	Baseline	$\tau = 0.96$	Crop Reduced
AOKVQA	71.44	72.23	10.39%
V*-Bench	75.90	86.38	14.13%
HR-Bench 8K	58.88	70.00	8.00%
HR-Bench 4K	67.50	72.50	10.00%
Average Δ	-	+9.35%	10.63%

Table 7: Evaluation under a fixed threshold ($\tau = 0.96$)

5 Conclusion

In this paper, we introduce AdaFocus, a novel training-free framework designed to tackle the dual challenges of perceptual redundancy and inefficient localization that MLLMs face when processing high-resolution tasks. AdaFocus intelligently determines when to crop via a confidence-based decision strategy, effectively circumventing redundant computation. Concurrently, it employs a semantic-guided localization technique to precisely identify where to focus, thereby overcoming the limitations of conventional attention mechanisms. Extensive experiments demonstrate that AdaFocus achieves state-of-the-art performance with high inference efficiency. Moreover, as a training-free plug-in, AdaFocus also exhibits strong generalization across diverse MLLMs architectures.

6 Limitations

Our work has two main limitations. First, the spatial precision of our semantic-guided localization is inherently limited by the resolution of the vision encoder’s attention map. While sufficient for most objects, pixel-level localization for extremely minute targets remains a challenge without higher-resolution feature maps. Second, as a plug-and-play module, AdaFocus relies on the foundational reasoning capabilities of the host MLLM. Errors stemming from the base model’s lack of domain-specific knowledge or severe logical hallucinations cannot be fully rectified solely through visual cropping.

References

- Jean-Baptiste Alayrac, Jeff Donahue, Pauline Luc, Antoine Miech, Iain Barr, Yana Hasson, Karel Lenc, Arthur Mensch, Katherine Millican, Malcolm Reynolds, and 1 others. 2022. Flamingo: a visual language model for few-shot learning. *Advances in neural information processing systems*, 35:23716–23736.
- Shuai Bai, Keqin Chen, Xuejing Liu, Jialin Wang, Wenbin Ge, Sibao Song, Kai Dang, Peng Wang, Shijie Wang, Jun Tang, and 1 others. 2025. Qwen2.5-vl technical report. *arXiv preprint arXiv:2502.13923*.
- Zhe Chen, Jiannan Wu, Wenhai Wang, Weijie Su, Guo Chen, Sen Xing, Muyan Zhong, Qinglong Zhang, Xizhou Zhu, Lewei Lu, and 1 others. 2024. Internvl: Scaling up vision foundation models and aligning for generic visual-linguistic tasks. In *Proceedings of the IEEE/CVF conference on computer vision and pattern recognition*, pages 24185–24198.
- Gheorghe Comanici, Eric Bieber, Mike Schaekermann, Ice Pasupat, Noveen Sachdeva, Inderjit Dhillon, Marcel Blistein, Ori Ram, Dan Zhang, Evan Rosen, and 1 others. 2025. Gemini 2.5: Pushing the frontier with advanced reasoning, multimodality, long context, and next generation agentic capabilities. *arXiv:2507.06261*.
- Wenliang Dai, Junnan Li, Dongxu Li, Anthony Tiong, Junqi Zhao, Weisheng Wang, Boyang Li, Pascale N Fung, and Steven Hoi. 2023. Instructblip: Towards general-purpose vision-language models with instruction tuning. *Advances in neural information processing systems*, 36:49250–49267.
- Zhenkun Gao, Xuhong Wang, Xin Tan, and Yuan Xie. 2026. Tpru: Advancing temporal and procedural understanding in large multimodal models. *arXiv preprint arXiv:2602.18884*.
- Arian Hosseini, Xingdi Yuan, Nikolay Malkin, Aaron Courville, Alessandro Sordani, and Rishabh Agarwal. 2024. V-star: Training verifiers for self-taught reasoners. *Preprint*, arXiv:2402.06457.
- Aaron Hurst, Adam Lerer, Adam P Goucher, Adam Perelman, Aditya Ramesh, Aidan Clark, AJ Ostrow, Akila Welihinda, Alan Hayes, Alec Radford, and 1 others. 2024. Gpt-4o system card. *arXiv:2410.21276*.
- Sanghwan Kim, Rui Xiao, Stephan Alaniz, Yongqin Xian, and Zeynep Akata. 2025. Training-free uncertainty guidance for complex visual tasks with mllms. *arXiv preprint arXiv:2510.00705*.
- Jaeseong Lee, Yeeun Choi, Heechan Choi, Hanjung Kim, and Seonjoo Kim. 2025. A training-free, task-agnostic framework for enhancing mllm performance on high-resolution images. *arXiv preprint arXiv:2507.10202*.
- Ming Li, Keyu Chen, Ziqian Bi, Ming Liu, Benji Peng, Qian Niu, Junyu Liu, Jinlang Wang, Sen Zhang, Xuanhe Pan, and 1 others. 2024a. Surveying the mllm landscape: A meta-review of current surveys. *arXiv preprint arXiv:2409.18991*.
- Yifan Li, Yifan Du, Kun Zhou, Jinpeng Wang, Wayne Xin Zhao, and Ji-Rong Wen. 2023. Evaluating object hallucination in large vision-language models. *arXiv preprint arXiv:2305.10355*.
- Yunxin Li, Zhenyu Liu, Zitao Li, Xuanyu Zhang, Zhenran Xu, Xinyu Chen, Haoyuan Shi, Shenyan Jiang, Xintong Wang, Jifang Wang, and 1 others. 2025. Perception, reason, think, and plan: A survey on large multimodal reasoning models. *arXiv preprint arXiv:2505.04921*.
- Zhang Li, Biao Yang, Qiang Liu, Zhiyin Ma, Shuo Zhang, Jingxu Yang, Yabo Sun, Yuliang Liu, and Xiang Bai. 2024b. Monkey: Image resolution and text label are important things for large multi-modal models. In *proceedings of the IEEE/CVF conference on computer vision and pattern recognition*, pages 26763–26773.
- Haotian Liu, Chunyuan Li, Yuheng Li, Bo Li, Yuanhan Zhang, Sheng Shen, and Yong Jae Lee. 2024. Llava-next: Improved reasoning, ocr, and world knowledge.
- Haotian Liu, Chunyuan Li, Qingyang Wu, and Yong Jae Lee. 2023. Visual instruction tuning. *Advances in neural information processing systems*, 36:34892–34916.
- Ziyu Liu, Yuhang Zang, Yushan Zou, Zijian Liang, Xiaoyi Dong, Yuhang Cao, Haodong Duan, Dahua Lin, and Jiaqi Wang. 2025. Visual agentic reinforcement fine-tuning. *arXiv preprint arXiv:2505.14246*.
- Alexander Neubeck and Luc Van Gool. 2006. Efficient non-maximum suppression. In *18th international conference on pattern recognition (ICPR'06)*, volume 3, pages 850–855. IEEE.
- OpenAI. 2025. Thinking with images. <https://openai.com/index/thinking-with-images/>.
- Alec Radford, Jong Wook Kim, Chris Hallacy, Aditya Ramesh, Gabriel Goh, Sandhini Agarwal, Girish Sastry, Amanda Askell, Pamela Mishkin, Jack Clark, and 1 others. 2021. Learning transferable visual models from natural language supervision. In *International conference on machine learning*, pages 8748–8763. PMLR.
- Dustin Schwenk, Apoorv Khandelwal, Christopher Clark, Kenneth Marino, and Roozbeh Mottaghi. 2022. A-okvqa: A benchmark for visual question answering using world knowledge. In *European conference on computer vision*, pages 146–162. Springer.
- Haozhan Shen, Kangjia Zhao, Tiancheng Zhao, Ruochen Xu, Zilun Zhang, Mingwei Zhu, and Jianwei Yin. 2025. Zoomeye: Enhancing multimodal llms with human-like zooming capabilities through

- tree-based image exploration. In *Proceedings of the 2025 Conference on Empirical Methods in Natural Language Processing*, pages 6613–6629.
- Zhaochen Su, Linjie Li, Mingyang Song, Yunzhuo Hao, Zhengyuan Yang, Jun Zhang, Guanjie Chen, Jiawei Gu, Juntao Li, Xiaoye Qu, and 1 others. 2025a. Open-thinking: Learning to think with images via visual tool reinforcement learning. *arXiv:2505.08617*.
- Zhaochen Su, Peng Xia, Hangyu Guo, Zhenhua Liu, Yan Ma, Xiaoye Qu, Jiaqi Liu, Yanshu Li, Kaide Zeng, Zhengyuan Yang, and 1 others. 2025b. Thinking with images for multimodal reasoning: Foundations, methods, and future frontiers. *arXiv:2506.23918*.
- Haozhe Wang, Alex Su, Weiming Ren, Fangzhen Lin, and Wenhui Chen. 2025a. Pixel reasoner: Incentivizing pixel-space reasoning with curiosity-driven reinforcement learning. *arXiv preprint arXiv:2505.15966*.
- Weiyun Wang, Zhangwei Gao, Lixin Gu, Hengjun Pu, Long Cui, Xingguang Wei, Zhaoyang Liu, Linglin Jing, Shenglong Ye, Jie Shao, and 1 others. 2025b. Internvl3.5: Advancing open-source multimodal models in versatility, reasoning, and efficiency. *arXiv:2508.18265*.
- Wenbin Wang, Liang Ding, Minyan Zeng, Xiabin Zhou, Li Shen, Yong Luo, Wei Yu, and Dacheng Tao. 2025c. Divide, conquer and combine: A training-free framework for high-resolution image perception in multimodal large language models. In *Proceedings of the AAAI Conference on Artificial Intelligence*, volume 39, pages 7907–7915.
- Jason Wei, Xuezhi Wang, Dale Schuurmans, Maarten Bosma, Fei Xia, Ed Chi, Quoc V Le, Denny Zhou, and 1 others. 2022. Chain-of-thought prompting elicits reasoning in large language models. *Advances in neural information processing systems*, 35:24824–24837.
- Penghao Wu and Saining Xie. 2024. V?: Guided visual search as a core mechanism in multimodal llms. In *Proceedings of the IEEE/CVF Conference on Computer Vision and Pattern Recognition*, pages 13084–13094.
- Jiarui Zhang, Mahyar Khayatkhoei, Prateek Chhikara, and Filip Ilievski. 2023. Towards perceiving small visual details in zero-shot visual question answering with multimodal llms. *arXiv preprint arXiv:2310.16033*.
- Jiarui Zhang, Mahyar Khayatkhoei, Prateek Chhikara, and Filip Ilievski. 2025. Mllms know where to look: Training-free perception of small visual details with multimodal llms. *arXiv preprint arXiv:2502.17422*.
- Ziwei Zheng, Michael Yang, Jack Hong, Chenxiao Zhao, Guohai Xu, Le Yang, Chao Shen, and Xing Yu. 2025. Deepeyes: Incentivizing "thinking with images" via reinforcement learning. *arXiv:2505.14362*.
- Deyao Zhu, Jun Chen, Xiaoqian Shen, Xiang Li, and Mohamed Elhoseiny. 2023. Minigpt-4: Enhancing vision-language understanding with advanced large language models. *arXiv preprint arXiv:2304.10592*.

A Implementation Details

Hyperparameter Settings. To validate the effectiveness of our approach, we integrate the AdaFocus framework with two widely-used open-source models: Qwen2.5VL-3B(Bai et al., 2025) and LLaVA-1.5-7B(Zhang et al., 2023). In our experiments, we set the maximum input resolution for Qwen to 3,211,264 pixels. All experiments are conducted on NVIDIA H200 GPUs.

B Prompt Settings

We leverage a few-shot prompt to guide the model in decoupling the original query and extracting the key semantic target, denoted as `<target>`. This is achieved by providing several examples to illustrate the extraction process.

Target Extraction Prompt

Question Template:

Based on the question, identify ONLY the primary, physical objects or subjects mentioned. Do not include adjectives, locations, or states.

Please respond using `<Reson>` and `<target>` tags.

Guidelines:

- A 'target' must be a simple, concrete noun (e.g., 'car', 'person', 'table').
- For multiple distinct subjects, separate them with a comma (e.g., 'cat, dog').

Question: What is the brand name on the laptop?

Response: `<Reson>`The question asks about a brand name found on a laptop. The core physical subject is the laptop.`</Reson><target>laptop</target>`

Question: How many people are wearing hats in the image?

Response: `<Reson>`The question asks to count people who are wearing hats. The primary subjects are people and hats.`</Reson><target>people, hats</target>`

Question: Is the cat on the left or right side of the wooden chair?

Response: `<Reson>`The question asks about the position of a cat relative to a wooden chair. The core physical subjects are the cat and the chair.`</Reson><target>cat, wooden chair</target>`

Question: What kind of food is on the white plate?

Response: `<Reson>`The question asks about the type of food on a plate. The primary physical subjects are the food and the plate.`</Reson><target>food, white plate</target>`

Question: What is the man in the blue shirt holding in his hand?

Response: `<Reson>`The question asks about an object held by a man. The core physical subjects are the man and the object he is holding.`</Reson><target>man, object</target>`

Question: What time is displayed on the clock on the wall?

Response: `<Reson>`The question asks for the time

displayed on a clock. The core physical subject is the clock.`</Reson><target>clock</target>`

C Dataset and Benchmark Statistics

To comprehensively evaluate our model’s performance across various dimensions, we first select the AOKVQA(Schwenk et al., 2022) and POPE(Li et al., 2023) datasets to assess its general reasoning capabilities on knowledge-intensive tasks. Furthermore, we introduce two highly challenging high-resolution datasets as our core benchmarks. The first is V*-Bench, which features an average image resolution of 2246×1582 and focuses on sub-tasks such as attribute recognition and spatial reasoning. The second is HR-Bench(Wang et al., 2025c). Its original version, HR-Bench8K, features an average image resolution as high as 7680 pixels on its longer side and comprises two main evaluation tracks: Fine-grained Single-instance Perception (FSP) and Fine-grained Cross-instance Perception (FCP). The HR-Bench4K version used in our experiments is generated by cropping the original 8K images centered on key objects.

Both high-resolution benchmarks are rich in visual elements, posing a significant challenge to a model’s ability to capture minute and often imperceptible fine-grained features. This makes them ideal for validating the effectiveness of our proposed cropping strategy, which is guided by spatial attention distributions. During implementation, to prevent cropped regions from becoming impractically small and devoid of meaningful context, we enforce a larger minimum bounding box size when processing these high-resolution images.

D Analysis of λ

In the utility function

$$J_{\lambda}(\tau) = \text{TPR}(\tau) - \lambda \cdot \text{FPR}(\tau), \quad (5)$$

the hyperparameter λ serves as a cost-weighting factor that balances the expected benefit of correctly triggering the cropping operation against the potential risk of unnecessary or ineffective cropping. Specifically, larger values of λ impose stronger penalties on false-positive decisions, encouraging a more conservative cropping policy, whereas smaller values favor more aggressive triggering to capture fine-grained visual details.

Effect of λ on the Decision Boundary. Varying λ systematically shifts the optimal decision thresh-

old τ , thereby controlling the trade-off between recall-oriented and precision-oriented behaviors. In our formulation, lower decision scores indicate a higher need for cropping, and cropping is triggered when the score falls below the threshold. Accordingly, as λ increases, the optimal threshold generally decreases, shrinking the triggering region and reducing the frequency of cropping, which improves computational efficiency. Conversely, smaller λ values expand the triggering region by adopting a higher threshold, enabling more frequent cropping at the cost of increased redundancy.

Practical Considerations. In practice, λ can be selected according to application-specific preferences between computational efficiency and potential performance gains. When representative validation data are available, λ may be tuned to maximize validation performance. In open-domain settings where such data are unavailable, moderate values of λ provide a stable and effective default choice.

E Methodology for Attention-Guided Cropping

Our approach to generating fine-grained crops involves a two-stage process. First, we acquire a target-specific attention map from the Vision-Language Model (VLM). Second, we use this map to determine an optimal bounding box via an adaptive algorithm.

E.1 Attention Map Acquisition

To isolate visual regions relevant to a target entity, we extract attention scores from the VLM’s Transformer architecture.

Implementation for Qwen2.5-VL For the Qwen2.5-VL model, we extract attention scores from **Layer 22**. To identify the query token, we first tokenize the target string (e.g., "white car") and locate its corresponding token ID sequence within the full prompt. The *last token* of this sequence is designated as the query. We found empirically that the raw attention map generated directly from this query token provided a sufficiently strong and clean signal for localization. The results presented in this paper are therefore based on this direct, target-specific attention map, which is reshaped into a 2D grid.

Implementation for LLaVA-1.5 For LLaVA-1.5, we use attention weights from **Layer 14**. The

model processes a 336×336 resolution image into a 24×24 grid of 576 image tokens. The target identification process focuses on the *final word* of the target phrase (e.g., "apple" from "the red apple"). *All tokens* comprising this final word are used as a composite query, and their attention scores are averaged to create a stable representation.

E.2 Adaptive Bounding Box Generation

We employ a universal adaptive algorithm to generate the bounding box. This method is designed to capture the object’s full extent rather than merely a single point of high attention.

Multi-Scale Window Search The algorithm iterates through a predefined set of scaling ratios (e.g., $[1, 1.2, \dots, 2]$). For each ratio r , a candidate window size is calculated by scaling an adaptive base dimension. This base dimension is determined by the input image’s resolution: it is set to 224×224 for images with a longer side below 1792 pixels, while for those at or exceeding this threshold, the base size is increased to 448×448 ($2 \times$ base) to ensure a sufficient field of view. The final candidate window, scaled by the ratio r , is then translated into corresponding dimensions on the attention map’s grid.

Aggregated Attention Scoring For each candidate window size, a sliding window traverses the attention map. At each position, the sum of all attention scores within the window is calculated, producing an "aggregated attention score map" for that scale.

Sharpness-based Scale Selection To select the optimal scale, we use a sharpness heuristic. For each scale, we identify the window with the maximum aggregated score. We then compute a **sharpness score** by calculating the difference between this peak score and the average score of its four adjacent, non-overlapping windows. This metric prioritizes crops where the target is highly distinct from its immediate surroundings.

Final Bounding Box Calculation The scaling ratio and window position that yield the highest sharpness score are selected as optimal. These coordinates from the attention grid are then mapped back to the original image’s pixel space. A final check ensures the bounding box coordinates (x_1, y_1, x_2, y_2) remain within the image boundaries.

F Evaluation on the Qwen3-VL Backbone

To validate the scalability and zero-shot generalization of our AdaFocus framework on the latest state-of-the-art vision-language models, we integrated it with the newly released **Qwen3-VL-4B** backbone.

We tested the model primarily on high-resolution and detail-heavy benchmarks where standard global-view perception often falls short. As shown in [Table 8](#), AdaFocus demonstrates consistent improvements over the baseline across all metrics: +0.88% on HR-Bench 4K (74.88% vs. 74.00%), +1.50% on HR-Bench 8K (69.25% vs. 67.75%), and +1.58% on V*-Bench (85.34% vs. 83.76%). These results confirm that our semantic-guided cropping strategy generalizes effectively to modern, advanced multimodal architectures without requiring any additional training or structural modifications.

Model (Qwen3-VL-4B)	HR 4K	HR 8K	V*-Bench
Baseline	74.00%	67.75%	83.76%
AdaFocus	74.88%	69.25%	85.34%
Δ	+0.88%	+1.50%	+1.58%

Table 8: Performance of AdaFocus with Qwen3-VL-4B.

G Detailed Performance Analysis on V*-Bench

While AdaFocus demonstrates strong performance across most benchmarks, we provide a deeper analysis of its behavior on V*-Bench, focusing on the specific challenges posed by representation constraints and complex spatial reasoning tasks.

Resolution and Representation Constraints. LLaVA-v1.5 processes images at a fixed 336×336 resolution, which inherently restricts spatial granularity. V*-Bench contains numerous extremely small objects and fine-grained visual targets. Under such low-resolution settings, attention maps may exhibit localization drift or insufficient precision, occasionally degrading the quality of the generated bounding regions. This explanation is corroborated by the significantly stronger performance observed when using the Qwen2.5-VL backbone, which supports dynamic high-resolution inputs (up to 3.2M pixels). The improved spatial fidelity of Qwen2.5-VL leads to more reliable attention localization and, consequently, highly accurate cropping decisions.

Efficiency vs. Spatial Reasoning Trade-off. V*-Bench heavily features spatial reasoning and visual search queries, such as determining the relative positions of distant objects. While AdaFocus successfully localizes multiple individual targets, it generates relatively tight bounding boxes around them. When objects are far apart, cropping tightly around them may inadvertently discard the surrounding contextual information necessary for inferring relational tasks.

In contrast, search-based methods like ZoomEyes utilize a recursive tree-search: they iteratively split the image into sub-regions, verify targets, and merge confident regions into a single large composite image. This exhaustive approach makes them more robust for complex spatial queries but incurs massive computational overhead (as demonstrated in our efficiency analysis, ZoomEyes suffers from an approximately $4.0\times$ latency increase). Overall, AdaFocus maintains competitive average performance while operating significantly faster. The performance gap on specific V*-Bench spatial queries primarily reflects a deliberate trade-off between inference efficiency and exhaustive spatial search, rather than a fundamental limitation of our semantic-guided localization.

H Case Study

To provide a qualitative understanding of our AdaFocus framework, we visualize representative examples from our benchmarks. These cases, shown in [Figure 7](#) through [Figure 10](#), illustrate the model’s ability to locate fine-grained details through attention-guided cropping, as well as a failure case that highlights current limitations.

Fine-grained Attribute Recognition. In the sailboat example ([Figure 8](#)), the user asks, "What kind of animal is on the blue sail?" In the original high-resolution image, the logo on the sail is minute and easily obscured by the surrounding water. Our model successfully identifies "Blue Sail" as the semantic target. The generated attention map accurately localizes the specific sail, and the subsequent cropping operation zooms in to reveal the spider logo clearly. This allows the model to answer "spider" correctly, whereas a standard model processing the resized full image would likely miss this low-pixel detail.

Small Object Perception. In the winter street scene (Figure 7), the query asks for the color of the bag carried by a pedestrian. The bag is a small, low-contrast object within a complex background. AdaFocus extracts "Bag" as the target and focuses the attention mechanism on the pedestrian's hand. The cropped region preserves the color information (purple), enabling the model to distinguish it from the dark clothing and gray surroundings. This demonstrates the framework's effectiveness in enhancing perception for small, incidental objects.

Spatial Reasoning with Multiple Targets. The park scene example (Figure 9) demonstrates the model's capability in handling spatial relationships. The question asks, "Is the baby stroller on the left or right side of the person in orange?" Here, the target extraction module identifies two distinct subjects: "Baby stroller" and "Person in orange." The attention mechanism successfully highlights both regions despite the cluttered background. By cropping the area that encompasses both the person and the stroller, the model maintains the necessary spatial context to determine that the stroller is on the right side.

Failure Case Analysis. Figure 10 illustrates a limitation in our current semantic extraction strategy. The question asks, "What is the dog trying to catch?" The few-shot extraction prompt identifies "dog" as the primary physical subject. Consequently, the attention mechanism and cropping focused exclusively on the dog. However, the answer ("Frisbee") lies high in the air, outside the cropped region. Because the extracted target did not include the potential object of the action, the cropped view lost the critical visual information required to answer the question. This suggests that for action-oriented queries, future work should consider incorporating gaze following or interaction inference into the cropping logic.

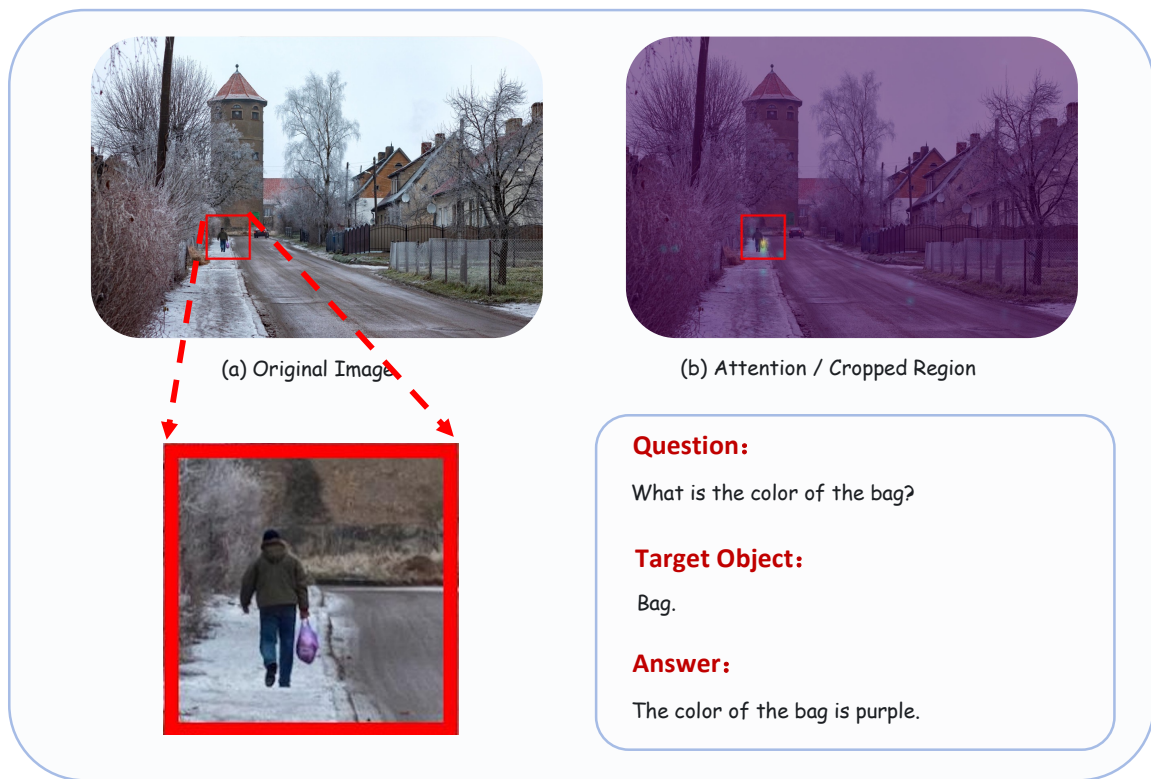


Figure 7: **Small Object Perception.** AdaFocus targets the "Bag" and crops the region around the pedestrian, allowing the model to identify the purple color despite the complex background.

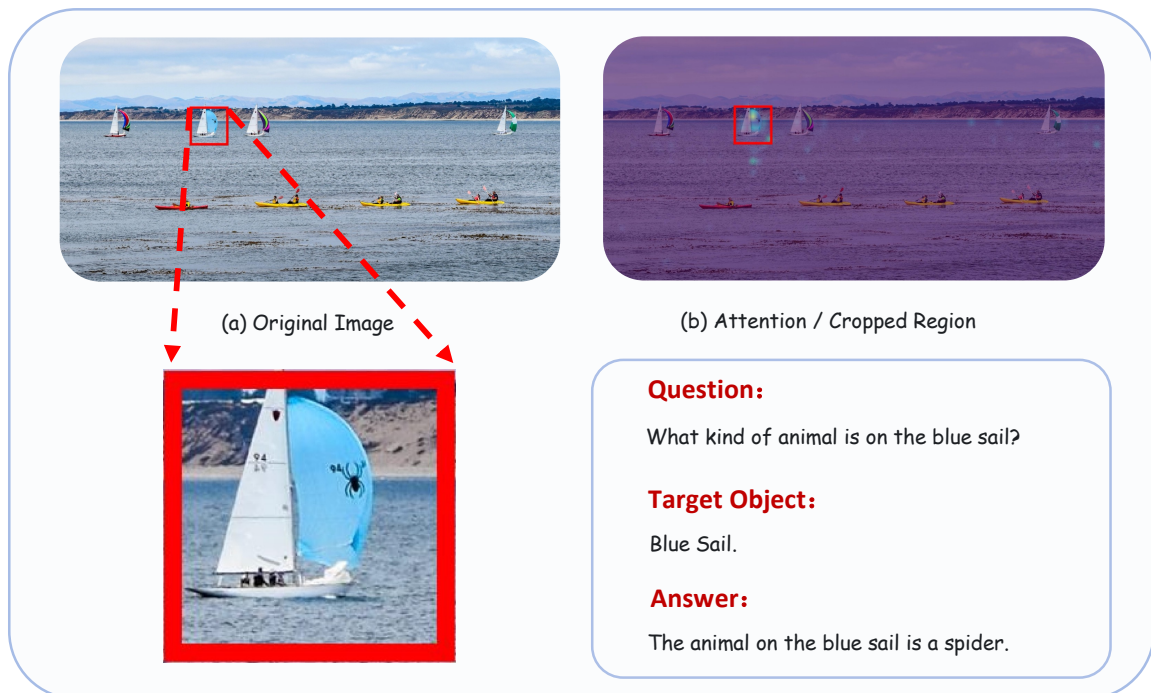


Figure 8: **Fine-grained Attribute Recognition.** The model successfully identifies the "Blue Sail" and crops the image to reveal the spider logo, answering the question correctly.



Figure 9: **Spatial Reasoning with Multiple Targets.** The model attends to both the "Baby stroller" and the "Person in orange," cropping a region that preserves their relative spatial position.

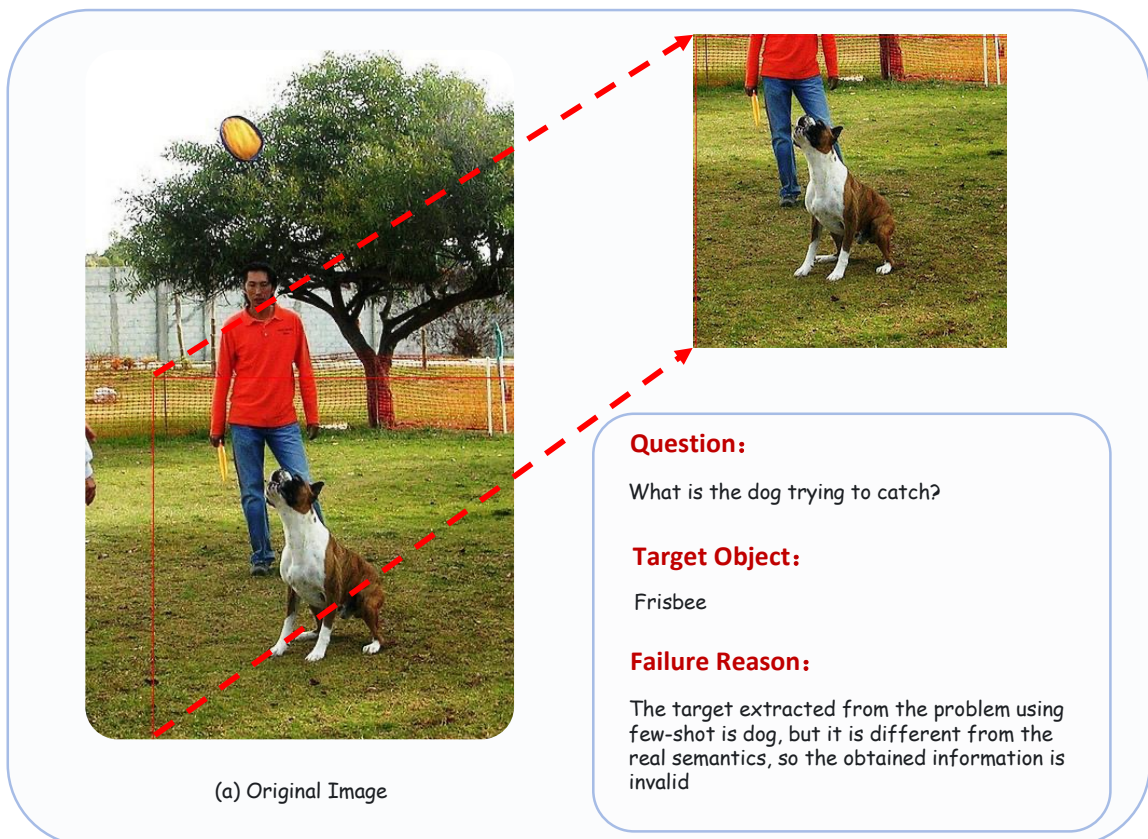


Figure 10: **Failure Case Analysis.** A limitation where the target "dog" is correctly identified, but the object of interest (the frisbee) is outside the cropped region due to lack of action context.